Infrared Multiple Photon Dissociation Spectroscopy of Cationized Asparagine: Effects of Metal Cation Size on Gas-Phase Conformation

A. L. Heaton,[†] V. N. Bowman,[†] J. Oomens,[‡] J. D. Steill,[‡] and P. B. Armentrout*,[†]

Department of Chemistry, University of Utah, Salt Lake City, Utah 84112 and FOM Institute for Plasma Physics "Rijnhuizen", Edisonbaan 14, 3439 MN Nieuwegein, The Netherlands

Received: January 27, 2009; Revised Manuscript Received: March 17, 2009

Gas-phase structures of cationized asparagine (Asn) including complexes with Li^+, Na^+, K^+, Rb^+, Cs^+, and Ba^{2+}, as well as protonated Asn, are examined by infrared multiple photon dissociation (IRMPD) action spectroscopy utilizing light generated by a free electron laser. Experimental spectra for the alkali metal cation complexes exhibit systematic trends, whereas spectra for Ba^{2+}(Asn) and H^+(Asn) are more distinct. To identify the structures formed experimentally, measured IRMPD spectra are compared to spectra calculated at a B3LYP/6-311+G(d,p) level with several effective core potentials and basis sets evaluated for the heavy metal systems. The dominant conformation ascertained for complexes with the smaller metal cations, Li^+(Asn) and Na^+(Asn), is a charge-solvated, tridentate [N,CO,CO] structure that binds the metal cation with the amine group of the amino acid backbone and to the carbonyl oxygen atoms of the backbone and amino acid side chain. For the larger alkali metal cation complexes, K^+(Asn), Rb^+(Asn), and Cs^+(Asn), an additional charge-solvated, tridentate [COOH,CO] structure that binds the metal cation with the two oxygen atoms of the backbone carboxylic acid group and the carbonyl oxygen atom of the Asn side chain may also be present. The Ba^{2+}(Asn) spectrum is characteristic of a single charge-solvated [N,CO,CO] conformation, in contrast to Gly, Trp, Arg, Gln, Pro, Ser, Val, and Glu, which all take on a zwitterionic structure when complexed to Ba^{2+}. In no case do the cationized Asn complexes show definitive evidence of forming a zwitterionic structure in the complexes studied here. For H^+(Asn), a mixture of two [N,CO] structures, which differ only in the orientation the side chain and are calculated to be nearly identical in energy, explains the experimental spectrum well.

Introduction

Complexes of asparagine (Asn) with sodium cations,[1] potassium cations,[2] and protons[3] have previously been investigated using guided ion beam mass spectrometry. For the Na^+ and K^+ complexes,[1,2] quantitative alkali-metal bond dissociation energies (BDEs) were determined by collision-induced dissociation (CID) and found to be consistent with theoretical values predicted for the ground-state (GS) conformation, a charge-solvated tridentate [N,CO,CO] structure (see nomenclature below) that binds the alkali metal cation with the amino nitrogen of the backbone and the two carbonyl oxygen atoms of the Asn ligand. For these M^+(Asn) complexes, [N,CO,CO] is calculated to lie well below ($\geq$5 kJ/mol) any other conformations, such that quantitative bond energy measurements are sufficient to determine the identity of the complexes formed experimentally. However, the energy gap between the ground state and first excited conformation of H^+(Asn)[3] is calculated to be significantly smaller. In fact, different levels of theory do not agree on the GS conformation, such that two potential GS H^+(Asn) complexes were considered in the analysis of the CID data. Interestingly, for CID of both the H^+(Asn)[3] and Na^+(Asn)[1,4,5] systems, reactions corresponding to deamidation of the reactant complexes are observed. Importantly, the deamidation reaction of Asn residues in proteins is the most commonly observed form of post-translational protein modification biologically.[6]

In order to assign ground-state conformations of these and related complexes more definitively, the present study involves the measurement of infrared multiple photon dissociation (IRMPD) action spectra for dissociation of Asn cationized by Li^+, Na^+, K^+, Rb^+, Cs^+, Ba^{2+}, and H^+. Identification of the conformations present is achieved by comparison to IR spectra derived from quantum chemical calculations of the low-lying structures of the cationized Asn complexes with optimized structures and vibrational frequencies determined at the B3LYP/6-311+G(d,p) level of theory. For the heavy metals, Rb, Cs, and Ba, several basis sets are examined and the present results used to evaluate their accuracy.

Experimental and Computational Section

Mass Spectrometry and Photodissociation. A home-built 4.7 T Fourier-transform ion cyclotron resonance (FTICR) mass spectrometer was used in these experiments and has been described in detail elsewhere.[7−9] Data acquisition and instrument control were performed using a PXI-based data station and an adapted version of the software developed by Heeren and coworkers.[10] Tunable radiation for the photodissociation experiments is generated by the free electron laser for infrared experiments (FELIX).[11] For the present experiments, spectra were recorded over the wavelength range from 19.4 (520 cm^{-1}) to 5.5 μm (1820 cm^{-1}). Pulse energies were around 50 mJ/macropulse of 5 μs duration, although they fell off to about 20 mJ toward the blue edge of the scan range. Complexes were irradiated for 3 s, corresponding to interaction with 15 macropulses. The fwhm bandwidth of the laser was typically 0.5% of the central wavelength. Asparagine was obtained from

* To whom correspondence should be addressed. E-mail: armentrout@chem.utah.edu.
† University of Utah.
‡ FOM Institute for Plasma Physics "Rijnhuizen".

10.1021/jp9008064 CCC: $40.75
Published on Web 04/15/2009

Aldrich. Metalated Asn complexes were formed by electrospray ionization using a Micromass Z-Spray source and a solution of 3.0 mM Asn and 0.5−1.0 mM alkali-metal chloride in 70%: 30% MeOH/H_2O solutions. Solution flow rates ranged from 15 to 30 μL/min, and the electrospray needle was generally held at a voltage of ~3.2 kV. Ions were accumulated in a hexapole trap for about 4 s prior to being injected into the ICR cell via a radiofrequency (rf) octopole ion guide. Electrostatic switching of the dc bias of the octopole, where a dc bias voltage is superimposed on the full length of all octopole rods, results in there being no change in the dc electric field along the axis of the ion guide. This dc bias switch decelerates the ions exiting the octopole so that they can be captured in the ICR cell without a gas pulse, so that collisional heating is avoided.[8]

Computational Details. In previous work, Heaton and Armentrout examined all likely conformers for Na^+(Asn),[1] K^+(Asn),[2] and H^+(Asn)[3] using a simulated annealing procedure that combines annealing cycles and quantum chemical calculations.[12] The same procedure is used here for the Li^+(Asn) complexes. Briefly, the AMBER program and the AMBER force field based on molecular mechanics[13] was used to search for possible stable structures in the conformational space of each system. All possible structures identified in this way were further optimized using NWChem[14] at the HF/3-21G level.[15,16] Unique structures for each system within 30 kJ/mol of the lowest energy structure (~10 for each complex) were further optimized using Gaussian 03[17] at the B3LYP/6-31G(d) level[18,19] with "loose" optimization (maximum step size of 0.01 au and an rms force of 0.0017 au) to facilitate convergence. Unique structures obtained from this procedure were then chosen for higher-level geometry optimizations and frequency calculations using density functional theory (DFT) at the B3LYP/6-311+G(d,p) level.[20,21] This level of theory has been shown to provide reasonably accurate structural descriptions of comparable cationized-ligand systems.[12,22−24] Single-point energy calculations were carried out for the 7−10 most stable structures at the B3LYP, B3P86, and MP2(full) levels using the 6-311+G(2d,2p) basis set.[20] Zero-point vibrational energy (ZPE) corrections were determined using vibrational frequencies calculated at the B3LYP/6-311+G(d,p) level scaled by a factor of 0.9804 to account for known inaccuracies.[25]

For the Rb^+, Cs^+, and Ba^{2+} complexes studied here, all conformations considered previously for Na^+(Asn)[1] and K^+(Asn)[2] were used as starting points for geometry and vibrational frequency calculations optimized at the B3LYP/HW*/6-311+G(d,p) level, where HW* indicates that Rb^+, Cs^+, and Ba^{2+} were described using the effective core potentials (ECPs) and valence basis sets of Hay and Wadt[26] (equivalent to the LANL2DZ basis set) with a single d polarization function added for the Rb^+ and Cs^+ cations (exponents of 0.24 and 0.19, respectively).[27] Relative energies were determined using single-point energies at the B3LYP, B3P86, and MP2(full) levels using the HW*/6-311+G(2d,2p) basis set. In previous work on serine complexes,[23] similar HW* calculations were performed for the K^+(Ser) complexes (with an exponent of 0.48 for the d polarization function on K^+) in order to assess the accuracy of the Hay-Wadt ECP/valence basis sets. It was found that vibrational frequencies calculated using the all electron vs the HW* basis sets on K^+ yield results that differ by an average of less than 0.03%. Hence, we did not perform HW* calculations on the Na^+(Asn) or K^+(Asn) complexes and conclude that the use of the HW* basis sets for the Rb^+ and Cs^+ systems should yield equivalent results to the all electron basis sets used for the smaller cations.

In addition to using the HW* basis sets on Rb^+, Cs^+, and Ba^{2+}, we also recalculated the geometries and single-point energies for the lowest energy conformers using the LANL08 basis sets (uncontracted versions of the HW basis set without the addition of polarization functions) but, unsurprisingly, found no significant changes in vibrational frequencies. Likewise, relative stabilities of the conformations calculated using LANL08 are the same as HW* within 0.4 kJ/mol for the B3LYP and B3P86 methods and within 5 kJ/mol for the MP2 method. We also examined results (geometries and single-point energies) calculated using Def2SVP basis sets for these three heavy metals, which are balanced basis sets of split valence quality, or Def2TZVP, triple-ζ valence quality for all elements.[28] These basis sets use ECPs developed by Leininger et al. for Rb and Cs[29] and by Kaupp et al. for Ba.[30] For the Rb^+(Asn) and Cs^+(Asn) complexes, vibrational frequencies calculated using the HW*/6-311+G(d,p), Def2SVP/6-311+G(d,p), and Def2TZVP basis sets are identical within about 2 cm^{-1} (average deviations of only 0.3%), although relative stabilities of the conformers change slightly, as discussed further below. For the Ba^{2+}(Asn) complexes, more distinct changes between the HW/6-311+G(d,p) and the Def2SVP/6-311+G(d,p) and the Def2TZVP results are observed in the predicted frequencies, probably because the HW basis set was not augmented with a polarization function. Finally, results using the CRENBL basis set and ECP on Ba[31] and 6-311+G(2d,2p)//6-311+G(d,p) on the other elements were also evaluated for the Ba^{2+}(Asn) complexes. As noted previously, calculations of the vibrational spectra of complexes of Ba^{2+} with amino acids are more accurate when d shell basis functions on Ba are employed,[32] such as those found in the Def2SVP, Def2TZVP (which also includes an f polarization function), and CRENBL basis sets, whereas the HW/LANL basis sets have no d shell. The LANL08, Def2SVP, Def2TZVP, and CRENBL basis sets were obtained from the EMSL basis set exchange library.[33,34]

For all systems, vibrational frequencies and intensities were calculated using the harmonic oscillator approximation and numerical derivatives of the energy-minimized Hessian calculated at the levels of theory noted above. Frequencies were scaled by 0.975 as this scaling factor leads to good agreement between calculated and experimentally well-resolved peaks and is in accord with previous IRMPD studies as well.[32,35] Use of the 0.9804 scaling factor noted above led to discrepancies in the most prominent bands near 1600−1700 cm^{-1} of about 14 cm^{-1}, whereas the 0.975 scaling factor reduces the discrepancies to less than 4 cm^{-1}. For comparison to experiment, calculated vibrational frequencies are broadened using a 20 cm^{-1} fwhm Gaussian line shape.

Results and Discussion

IRMPD Action Spectroscopy. Photodissociation of Asn cationized with Li^+, Na^+, K^+, Rb^+, Cs^+, Ba^{2+}, and H^+ was examined. For metalated Asn complexes with K^+, Rb^+, and Cs^+, photodissociation results only in the loss of the intact ligand to form the atomic metal cation, reaction 1.

$$M^+(\text{Asn}) + h\nu \rightarrow M^+ + \text{Asn} \quad (1)$$

This result is consistent with the observation of intact ligand loss as the sole pathway observed in the CID spectra of K^+(Asn).[2] In contrast, Li^+(Asn), Na^+(Asn), Ba^{2+}(Asn), and H^+(Asn) display alternative decomposition pathways in the IRMPD spectra. For photodissociation of Li^+(Asn), products observed are formed in reactions 2−4, where the number in brackets indicates the mass to charge ratio of the product ion.

$$Li(Asn)[139] + h\nu \rightarrow Li^+(a\text{-}SA)[122] + NH_3 \quad (2)$$

$$\rightarrow Li^+(C_3H_5NO_2)[94] + CO + NH_3 \quad (3)$$

$$\rightarrow Li^+(C_3H_8N_2O)[95] + CO_2 \quad (4)$$

The major charged reaction product appears at *m/z* 122, which corresponds to deamidation of the Asn ligand. In analogy with the results for deamidation of Na^+(Asn),[4,5] this is believed to form a 5-membered heterocyclic ring product, lithiated 3-amino succinic anhydride, Li^+(a-SA). Subsequent loss of CO leads to a product at *m/z* 94, which has about one-half to one-third of the intensity of the *m/z* 122 product, except for the highest frequency band where the intensities are equal. A product at *m/z* 95 is also observed and likely corresponds to CO_2 loss from the initial complex. The intensity of this product ion ranges from one-half to equal to that of the *m/z* 94 product.

For Na^+(Asn), IRMPD leads to charged products appearing at *m/z* 138 and 66, reactions 5 and 6.

$$Na^+(Asn)[155] + h\nu \rightarrow Na^+(a\text{-}SA)[138] + NH_3 \quad (5)$$

$$\rightarrow Na^+(C_2H_5N)[66] + CO + CO_2 + NH_3 \quad (6)$$

The former product must be Na^+(a-SA), the deamidation product identified elsewhere.[4,5] The latter product, believed to be $Na^+(H_3C{-}CH{=}NH)$, results from sequential dissociation of Na^+(a-SA) by loss of CO + CO_2 and has an intensity that is less than 10% of the major signal at *m/z* 138 throughout the spectrum. This sequential formation of *m/z* 66 was not observed in the CID spectra of Na^+(Asn),[1] suggesting that this channel is relatively low in energy but entropically disfavored, such that its production is enhanced by the slow heating afforded by IRMPD. Interestingly, loss of the intact Asn ligand was observed in the CID spectra of Na^+(Asn) but is not observed in photodissociation, which may again be attributed to slower heating of the precursor ion, thereby favoring the lower energy deamidation channel.

For Ba^{2+}(Asn), photodissociation leads to reactions 7−9, where only the heavier of the two product ions formed in each process is observed.

$$Ba^{2+}(Asn)[135] + h\nu \rightarrow BaOH^+[155] + C_4H_7N_2O_2^+[115] \quad (7)$$

$$\rightarrow Ba^+C_2H_2NO_2[210] + CH_3CONH_3^+[60] \quad (8)$$

$$\rightarrow Ba^+C_4H_4NO_3[252] + NH_4^+[18] \quad (9)$$

In no case is the complementary product ion (*m/z* 115, 60, and 18) observed, presumably because these lighter product ions are not efficiently trapped given the high velocities resulting from Coulomb repulsion between the singly charged product ions. The relative intensity of the *m/z* 252 product is about twice that of *m/z* 210, which is about twice that of *m/z* 155.

For H^+(Asn), a detailed scheme for dissociation is presented elsewhere.[3] Here, photodissociation yields charged products appearing at *m/z* 87, $H_2N^+{=}CH{-}CH_2{-}C(O)NH_2$ from (H_2O + CO) loss, at *m/z* 116, H^+(a-SA) formed by deamidation, at *m/z* 74, $O{=}C{=}CH_2$ loss from H^+(a-SA), at *m/z* 70, $H_2N^+{=}CH{-}CH{=}CO$ formation by deamidation of *m/z* 87, and at *m/z* 44, $H_3C{-}CH{=}NH_2^+$ formation by CO and CO_2 loss from H^+(a-SA). Observation of the primary (H_2O + CO) loss and deamidation reaction pathways here is consistent with CID results for protonated asparagine,[3] where the former is the lowest energy process observed, consistent with it having the highest photodissociation intensity. The intensity of the *m/z* 116 product is generally about 20% of the *m/z* 87 product, except that its intensity in the highest frequency band is much smaller. The intensities of the *m/z* 44, 70, and 74 product ions are comparable to each other and smaller than the *m/z* 116 product, consistent with their identification as sequential reaction products. All these products, except for *m/z* 70, were observed in the CID of H^+(Asn).[3]

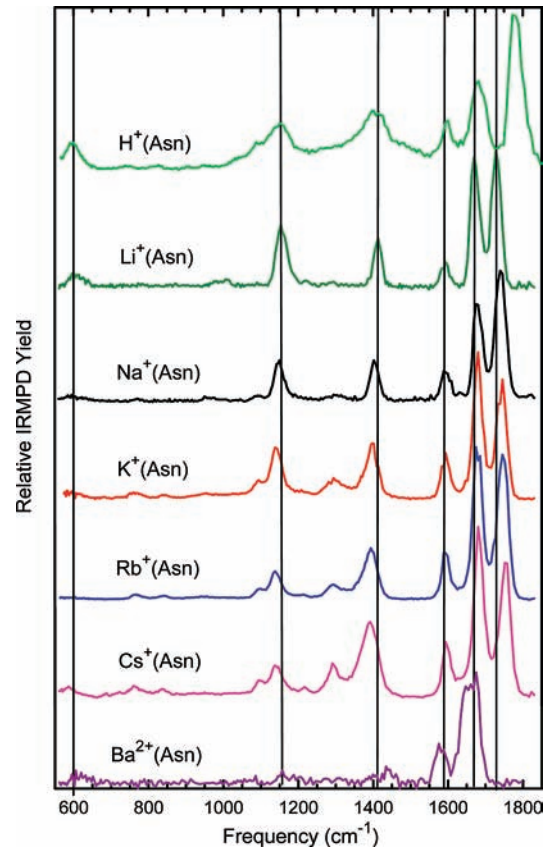

Figure 1. Infrared multiphoton dissociation action spectra of M^+(Asn) complexes where $M^+ = H^+$, Li^+, Na^+, K^+, Rb^+, Cs^+, and Ba^{2+}.

For the K^+, Rb^+, and Cs^+ complexes of Asn, IRMPD action spectra are taken from the relative intensity of the M^+ product ion as a function of laser wavelength and are shown in Figure 1, whereas in the Li^+, Na^+, Ba^{2+}, and H^+ complexes of Asn, the sum of all observed reaction pathways is shown. Linear corrections for laser power are additionally applied, which mainly affects the relative intensities observed at the highest laser frequencies. Comparison of the five spectra for the alkali metal complexes in Figure 1 shows that the six dominant features observed in the Li^+(Asn) spectrum (600, 1160, 1415, 1595, 1670, and 1730 cm^{-1}) are retained for all of the alkali metal cation complexes, although the features at 600 cm^{-1} for K^+(Asn) and Rb^+(Asn) are not clear unless viewed on an expanded scale (see below). The bands at 1670 and 1730 cm^{-1} shift to the blue as the alkali metal cation becomes heavier. In contrast, those at 1160 and 1415 cm^{-1} shift to the red, and the bands at 600 and 1595 cm^{-1} shift very little. New spectral features at 1100 and 1290 cm^{-1} begin to appear for the Na^+(Asn) spectra and become pronounced for the K^+, Rb^+, and Cs^+ complexes. Likewise, weak bands at 760 and 840 cm^{-1} appear for the latter three complexes.

The H^+(Asn) and Ba^{2+}(Asn) spectra shown in Figure 1 are somewhat more distinctive, in part because the presence of multiple decomposition pathways of high energy lead to low product intensities. The H^+(Asn) spectrum closely resembles a

broadened version of those of the alkali metal cation complexes, with the exception that the highest frequency band has blue shifted to a unique feature at 1775 cm^{-1}. In contrast, Ba^{2+} exhibits broad bands at 1440, 1575, and 1660 cm^{-1}, with weak features at 600 and 1155 cm^{-1}.

Theoretical Results. A detailed discussion of the structures of asparagine[1] and its cationized structures with Na^+, K^+, and H^+ can be found elsewhere.[1−3] As described above, Asn complexes with Rb^+, Cs^+, and Ba^{2+} were calculated here at the B3LYP/HW*/6-311+G(d,p) level starting with the structures of all low-lying sodiated and potassiated complexes located previously, a total of seven conformations, along with a tridentate zwitterionic structure similar to that located for other Ba amino acid complexes.[32] The lowest of these were also explored using other basis sets, as noted above. The nomenclature used to identify these different structural isomers is based on that established previously for Na^+(Asn)[1] and H^+(Asn).[3] Briefly, conformations of cationized Asn are identified by their metal binding site (or protonation site) in brackets, followed by a description of the ligand orientation, named by the series of dihedral angles starting from the carboxylic acid hydrogen of the backbone (or the analogous proton on NH_2 in zwitterionic structures) and going to the terminal side-chain nitrogen. The dihedral angles are distinguished as cis (c, for angles between 0° and 45°), gauche (g, 45° and 135°), or trans (t, 135° and 180°). Single-point energies including zero-point energy (ZPE) corrections calculated at three different levels of theory, relative to the lowest energy isomer, are given in Table 1 for the cationized Asn complexes. Because the relative Gibbs free energies at 298 K may be more relevant in the determination of the experimental distribution, these values are also listed in Table 1. Conversion from 0 K bond energies to 298 K free energies is accomplished using the rigid rotor/harmonic oscillator approximation with rotational constants and vibrational frequencies calculated at the B3LYP/6-311+G(d,p) and B3LYP/HW*/6-311+G(d,p) levels. Figure 2 shows the overall trends in the relative $\Delta_{298}G$ values, which are very similar to those of the relative Δ_0H values. B3P86 and MP2(full) levels of theory show similar trends as the B3LYP values in Figure 2.

At all three levels of theory, the ground state of neutral asparagine has a ctgg structure,[1] which is stabilized by four intramolecular hydrogen bonds: $OH\cdots N_{bb}H_2$ (1.897 Å), $HN_{bb}H\cdots OC_{sc}$ (2.223 Å), $HN_{sc}H\cdots OC_{sc}$ (2.498 Å), and $HN_{sc}H\cdots OC_{bb}$ (2.657 Å), where bb and sc indicate backbone and side-chain groups. The next highest energy structure, cttt, is stabilized by only the first three hydrogen bonds, 1.929, 2.499, and 2.498 Å, respectively, and lies 2.2−7.6 kJ/mol above the GS. Two other low-lying conformations (cggt and cgtg) have also been described and are found to lie within 9.5 kJ/mol of the GS at all levels of theory.[1] Each is additionally stabilized by three intramolecular hydrogen bonds. Figure 3 illustrates the low-lying metal binding orientations found for the metalated Asn complexes as exemplified by Rb^+(Asn) along with the zwitterionic structure of Ba^{2+}(Asn). Table 2 lists several important geometric parameters for each of the cationized Asn complexes. The ground-state structures for Li^+(Asn), Na^+(Asn), K^+(Asn), and Ba^{2+}(Asn) all have a tridentate [N,CO,CO]tggt binding orientation, whereas the calculated GS for Cs^+(Asn) rather has a tridentate [COOH,CO]ctgt binding arrangement. For Rb^+(Asn), the B3LYP and MP2(full) calculations find a [N,CO,CO] conformer to be the ground state, Table 1, whereas the B3P86 calculations predict a [COOH,CO] conformer as the ground state.

TABLE 1: Relative Energies at 0 K and Free Energies at 298 K (kJ/mol) of Low-Lying Conformers of Cationized Asn[a]

complex	structure	B3LYP	B3P86	MP2(full)
Li^+(Asn)	[N,CO,CO]tggt	0.0 (0.0)	0.0 (0.0)	0.0 (0.0)
	[N,OH,CO]tggt	25.4 (25.1)	26.7 (26.5)	22.8 (22.6)
	[CO,CO]cggt	25.7 (23.1)	25.1 (22.4)	38.1 (35.4)
	[N,CO,CO]cggt	27.9 (27.7)	28.0 (27.8)	29.6 (29.4)
	[CO,CO]tggt	33.2 (29.0)	35.5 (31.3)	44.8 (40.6)
	[CO,CO]ctgg	34.3 (33.0)	33.0 (31.6)	42.7 (41.3)
	[CO_2^-]ctgt	44.4 (42.1)	38.4 (36.2)	44.5 (42.3)
Na^+(Asn)	[N,CO,CO]tggt	0.0 (0.0)	0.0 (0.0)	0.0 (0.0)
	[CO_2^-ctgt	21.4 (20.7)	15.8 (15.0)	23.5 (22.7)
	[CO,CO]ctg$_+$g$_+$	22.2 (19.4)	21.6 (18.9)	32.5 (29.7)
	[CO,CO]ctg$_-$g$_-$	23.7 (22.4)	20.9 (19.5)	27.7 (26.3)
	[CO,CO]cggt	24.0 (19.5)	22.2 (17.7)	31.7 (27.1)
	[CO_2^-]cgtt	24.9 (23.4)	20.2 (18.7)	29.1 (27.6)
	[N,CO,CO]cggt	28.8 (28.3)	29.2 (28.7)	30.8 (30.3)
K^+(Asn)	[N,CO,CO]tggt	0.0 (0.0)	0.0 (0.0)	0.0 (0.0)
	[COOH,CO]cggt	8.0 (7.3)	4.9 (4.2)	7.3 (6.6)
	[CO_2^-]ctgt	12.4 (11.3)	6.9 (5.8)	17.7 (16.7)
	[CO_2^-]cgtt	14.4 (13.1)	11.8 (10.5)	23.3 (22.0)
	[CO,CO]ctgg	15.5 (18.2)	15.0 (17.7)	27.5 (30.2)
	[CO,CO]cggt$_-$	15.7 (13.9)	14.6 (12.7)	23.2 (21.3)
	[CO,CO]cggt$_+$	16.4 (13.4)	15.8 (12.8)	23.0 (20.1)
Rb^+(Asn)	[N,CO,CO]tggt	*0.0 (0.0)*	*2.4 (2.3)*	*0.0 (0.0)*
	[COOH,CO]ctgt	*0.7 (0.7)*	*0.0 (0.0)*	*1.3 (1.4)*
	[CO_2^-]ctgt	*8.7 (7.8)*	*6.0 (5.1)*	*19.2 (18.3)*
	[CO,CO]cggg	*10.9 (8.5)*	*12.7 (10.2)*	*17.9 (15.5)*
	[CO,CO]cggt	*11.6 (9.6)*	*12.9 (10.9)*	*20.8 (18.8)*
	[CO_2^-]cgtt	*12.5 (11.4)*	*10.9 (9.7)*	*24.9 (23.8)*
	[CO,CO]ctgg	*12.7 (8.2)*	*14.2 (9.6)*	*26.0 (21.4)*
Cs^+(Asn)	[COOH,CO]ctgt	*0.0 (0.0)*	*0.0 (0.0)*	*0.0 (0.0)*
	[N,CO,CO]tggt	*3.9 (3.3)*	*6.9 (6.3)*	*2.6 (2.0)*
	[CO_2^-]ctgt	*11.0 (9.9)*	*8.9 (7.9)*	*20.9 (19.9)*
	[CO,CO]cggg	*11.8 (8.9)*	*14.2 (11.4)*	*16.7 (13.9)*
	[CO,CO]ctgt	*12.3 (9.8)*	*13.7 (11.2)*	*21.0 (18.5)*
	[CO,CO]cggt	*13.1 (10.5)*	*15.1 (12.6)*	*20.7 (18.1)*
	[CO_2^-]cgtt	*14.8 (13.1)*	*13.8 (12.1)*	*26.6 (25.0)*
Ba^{2+}(Asn)	[N,CO,CO]tggt	*0.0 (0.0)*	*0.0 (0.0)*	*0.0 (0.0)*
	[CO_2^-,CO]cgct	*15.3 (14.8)*	*12.5 (12.0)*	*10.2 (9.7)*
	[N,CO,CO]cggt	26.8 (26.4)	*27.1 (26.6)*	*27.3 (26.8)*
	[CO,CO]ctgg	*30.5 (28.1)*	*30.7 (28.3)*	*39.0 (36.6)*
	[COOH,CO]cggt	*32.2 (32.3)*	*28.8 (28.9)*	*26.3 (26.4)*
	[CO_2^-]ctgt	*33.6 (30.2)*	*31.4 (28.0)*	*29.0 (25.7)*
	[CO_2^-]cgtt	*36.9 (32.9)*	*34.6 (30.6)*	*37.7 (33.7)*
	[N,OH,CO]tggt	*53.1 (52.5)*	*54.9 (54.3)*	*45.3 (44.7)*
H^+(Asn)	[N,CO]tgtt	0.0 (0.0)	0.0 (0.0)	0.5 (0.1)
	[N,CO]tcgt	2.4 (2.8)	1.5 (1.8)	0.0 (0.0)
	[N,CO]ttgt	10.7 (11.1)	10.5 (10.8)	7.0 (7.0)
	[N,CO]tttt	11.5 (10.1)	12.8 (11.4)	11.5 (9.7)
	[CO,CO]ctgt	30.1 (33.0)	24.5 (27.4)	39.6 (42.2)
	[N,CO]cgtt	36.1 (36.1)	36.6 (36.6)	37.2 (36.8)
	[CO,CO]cggt	42.3 (43.5)	38.7 (39.9)	45.0 (45.8)

[a] Free energies in parentheses. All values calculated at the level of theory indicated using the 6-311+G(2d,2p) basis set with structures and zero-point energies calculated at the B3LYP/6-311+G(d,p) level of theory. Values in italics use the HW* basis set on the metal.

It is useful to directly compare the geometries of the alkali metal cation complexes, as characterized in Table 2. As the [N,CO,CO]tggt complexes of the alkali metal cations vary from Li^+ to Cs^+, their ($M-O_{bb}$) and ($M-O_{sc}$) distances, where the latter are uniformly shorter by ~0.1 Å, are calculated to increase for the backbone oxygen from 1.98 to 2.32 to 2.67 to 2.92 to 3.13 Å, respectively, and for the side-chain oxygen from 1.87 to 2.23 to 2.58 to 2.83 to 3.05 Å, respectively. These changes directly reflect the increase in the ionic radius of the metal cation (0.70 Å for Li^+, 0.98 Å for Na^+, 1.33 Å for K^+, 1.49 Å for

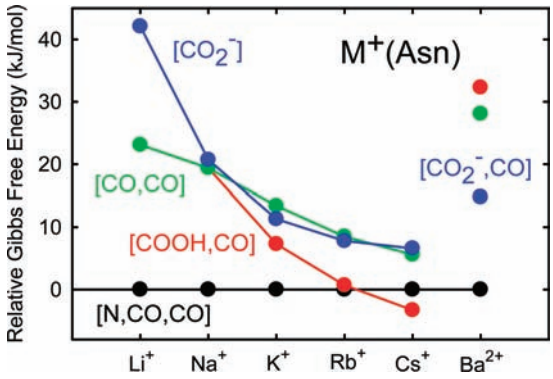

Figure 2. Gibbs free energies (kJ/mol) calculated at the B3LYP/HW*/6-311+G(d,p) level of theory (Table 1) of four conformations of M^+(Asn), where $M^+ = Li^+$, Na^+, K^+, Rb^+, Cs^+, and Ba^{2+}, as a function of the metal cation identity relative to the energy of the [N,CO,CO] conformer.

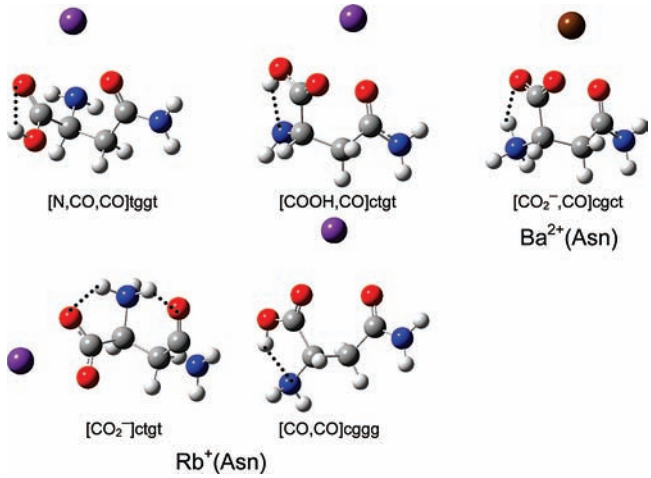

Figure 3. Structures of the Rb^+(Asn) complexes and the zwitterionic structure of Ba^{2+}(Asn) calculated at the B3LYP/HW*/6-311+G(d,p) level of theory. Dashed lines indicate hydrogen bonds.

Rb^+, and 1.69 Å for Cs^+)[36] coupled with the resultant decreasing charge density, which weakens the electrostatic interaction with asparagine. In contrast, the relative M−N distances for the alkali metal cationized [N,CO,CO]tggt structures increase by 0.39 Å for Na^+ compared to Li^+, by 0.46 Å for K^+ compared to Na^+, 0.32 Å for Rb^+ compared to K^+, and 0.32 Å for Cs^+ compared to Rb^+. These changes do not directly reflect the increase in the ionic radius and therefore indicate a weakening of the metal cation interaction with the amino group compared to the carbonyl groups as the metal cation size increases. This trend has previously been noted in our analysis of the interactions of Na^+(Gly)[12] and K^+(Gly),[22] as well as Na^+(Asn)[1] and K^+(Asn)[2] complexes. Additionally, the $\angle(NMO_{bb})$, $\angle(NMO_{sc})$, and $\angle(O_{bb}MO_{sc})$ bond angles of the alkali metal [N,CO,CO]tggt structures are found to decrease with increasing size of the metal cation, Table 2, which again reflects the changes associated with the metal cation size. Similar trends of decreasing ($M-O_{bb}$), ($M-O_{sc}$), and (M−OH) distances with increasing $\angle(OMO_{bb})$, $\angle(OMO_{sc})$, and $\angle(O_{bb}MO_{sc})$ bond angles are apparent for the [COOH,CO] structures observed in the K^+, Rb^+, and Cs^+ complexes of asparagine. Conformations differ slightly, cggt for K^+(Asn) versus ctgt for Rb^+(Asn) and Cs^+(Asn), because the OCCC dihedral angles (132°, 136°, and 139°, respectively) are close to the 135° borderline between our gauche and trans designations The relative energies of these conformers depend strongly on the metal identity, Figure 2, which also indicates that these structures collapse to the bidentate [CO,CO] structure for Li^+(Asn) and Na^+(Asn).

Two additional low-energy binding orientations of the cationized Asn complexes were identified, Figure 3. These [CO,CO] and [CO_2^-] arrangements are both bidentate and each remain at least 5 kJ/mol higher in energy than the ground-state conformer, Table 1. The [CO,CO] binding arrangements retain the metal cation interactions with the oxygen atoms of the backbone and side-chain carbonyls found in both [N,CO,CO] and [COOH,CO]. Because of the reduced steric constraints, these bidentate structures have M−O bond distances that are shorter by ∼0.07 Å than the [N,CO,CO]tggt conformer for all five metal cations. The lowest energy [CO,CO] conformer lies 22−36, 19−27, 12−22, 7−15, and 5−17 kJ/mol above [N,CO,CO]tggt for Li^+−Cs^+, respectively, Table 1. These changes in the relative energies with metal cation identity reflect the stronger binding to the smaller cations. The other bidentate binding arrangement is zwitterionic, [CO_2^-], where M^+ binds to the equivalent oxygen atoms of the backbone carboxylic group and the backbone amino group becomes protonated and hydrogen bound to the side-chain carbonyl, Figure 3. The relative energy of this conformation depends strongly on metal cation identity and most favorably occurs for each metal complex as [CO_2^-]ctgt, with a [CO_2^-]cgtt conformer somewhat higher in energy. The energy of this conformer for Li^+(Asn), Na^+(Asn), K^+(Asn), Rb^+(Asn), and Cs^+(Asn), respectively, is at least 36, 15, 6, 5, and 2 kJ/mol higher than [N,CO,CO]tggt, dropping by about 38 kJ/mol in relative stability in going from Li^+(Asn) to Cs^+(Asn), Figure 2. Trends in the ($M-O_{bb}$), ($M-O_{sc}$), and bond angles with metal cation are similar to those for the [N,CO,CO]tggt conformers.

We also explicitly looked for a tridentate [CO_2^-,CO] structure, directly analogous to the [COOH,CO] charge-solvated structure. This zwitterionic structure is very high energy for Li^+(Asn) and Na^+(Asn), lying 65−73 and 43−49 kJ/mol, respectively, above the ground state and 26−36 and 22−26 kJ/mol, respectively, above the [COOH,CO] charge-solvated analogue. For the K^+(Asn), Rb^+(Asn), and Cs^+(Asn) complexes, this structure collapses to the bidentate zwitterion, [CO_2^-], i.e., the side chain prefers to hydrogen bond to the protonated amino group rather than to the metal cation. This preference appears to be directed by lower steric strain in the bidentate structure.

The low-energy conformations found for the alkali metal complexes are also found to be low-energy structures of Ba^{2+}(Asn). The ionic radius of Ba^{2+} is 1.38 Å, slightly larger than K^+.[36] Consistent with this, the ($M-O_{bb}$), ($M-O_{sc}$), and (M−X) bond distances for each of the calculated structures of Ba^{2+}(Asn) are found to be slightly greater than those of the analogous K^+(Asn) conformer, Table 2 (where X is the amino nitrogen in [N,CO,CO], the hydroxyl oxygen in [COOH,CO], and the carboxylate oxygen hydrogen bound to the protonated amino group in [CO_2^-] and [CO_2^-,CO]). Likewise, the bond angles listed for Ba^{2+}(Asn) are slightly smaller than those of K^+(Asn), in agreement with the trends in metal cation size. However, because of the 2+ charge on Ba, the relative energies of the various conformers are more similar to those of Li^+(Asn) and Na^+(Asn) than to those of the heavier alkali cations, see Table 1 and Figure 2. Furthermore, in contrast to the alkali cation complexes, the lowest energy zwitterionic structure is tridentate, Ba^{2+}(Asn)[CO_2^-,CO]cgct. At all three levels of theory with the HW/6-311+G(d,p) basis set, Ba^{2+}(Asn)[N,CO,CO]tggt is at least 10 kJ/mol more stable than any other Ba^{2+}(Asn) structure.

Lastly, unique among all of the cationized Asn complexes is H^+(Asn). The GS conformation protonates the amino nitrogen

TABLE 2: Bond Distance (Å) and Bond Angles (deg) for Low-Energy Structures of Metalated Asparagine[a]

	$r(M-O_{bb})$						$r(M-X)$						$r(M-O_{sc})$					
conformer	Li^+	Na^+	K^+	Rb^+	Cs^+	Ba^{2+}	Li^+	Na^+	K^+	Rb^+	Cs^+	Ba^{2+}	Li^+	Na^+	K^+	Rb^+	Cs^+	Ba^{2+}
[N,CO,CO][b]	1.978	2.318	2.670	*2.918*	*3.133*	*2.709*	2.094	2.479	2.934	*3.252*	*3.570*	*2.995*	1.870	2.230	2.576	*2.826*	*3.045*	*2.609*
				2.856	**3.018**	**2.603**				**3.181**	**3.392**	**2.887**				**2.768**	**2.931**	**2.497**
[COOH,CO][c]	[d]	[d]	2.693	*2.949*	*3.163*	*2.748*	[d]	[d]	2.955	*3.169*	*3.384*	*2.966*	[d]	[d]	2.650	*2.942*	*3.189*	*2.664*
				2.871	**3.024**	**2.590**				**3.132**	**3.308**	**2.954**				**2.875**	**3.067**	**2.533**
[CO,CO]	1.817	2.214	2.558	*2.844*	*3.039*	*2.582*							1.819	2.228	2.576	*2.844*	*3.119*	*2.605*
				2.776	**2.953**											**2.776**	**2.944**	
$[CO_2^-]$[e]	1.937	2.295	2.641	*2.905*	*3.134*	*2.719*	1.943	2.299	2.650	*2.913*	*3.122*	*2.720*						
				2.850	**2.979**	**2.554**				**2.825**	**2.998**	**2.573**						
$[CO_2^-$,CO][e]	2.006	2.350	[f]	[f]	[f]	*2.721*	2.080	2.398	[f]	[f]	[f]	*2.780*	1.950	2.354	[f]	[f]	[f]	*2.723*
						2.576						**2.669**						**2.621**

	$\angle(XMO_{bb})$						$\angle(XMO_{sc})$						$\angle(O_{bb}MO_{sc})$					
conformer	Li^+	Na^+	K^+	Rb^+	Cs^+	Ba^{2+}	Li^+	Na^+	K^+	Rb^+	Cs^+	Ba^{2+}	Li^+	Na^+	K^+	Rb^+	Cs^+	Ba^{2+}
[N,CO,CO][b]	82.9	69.7	58.3	*52.4*	*47.7*	*57.6*	93.6	79.6	67.9	*61.6*	*56.3*	*64.0*	102.1	88.3	75.6	*69.1*	*63.7*	*73.2*
				53.6	**50.0**	**59.6**				**63.1**	**59.1**	**66.5**				**70.5**	**66.1**	**75.9**
[COOH,CO][c]	[d]	[d]	46.0	*42.4*	*39.6*	*45.3*	[d]	[d]	69.1	*64.1*	*60.1*	*64.7*	[d]	[d]	69.2	*63.0*	*58.6*	*66.6*
				43.1	**40.7**	**46.3**				**65.3**	**61.8**	**67.2**				**64.6**	**60.9**	**70.4**
[CO,CO]													168.8	84.4	71.5	*62.4*	*58.9*	*68.6*
																64.2	**60.2**	
$[CO_2^-]$[e]	69.8	58.4	50.3	*45.6*	*42.3*	*48.4*												
				46.7	**44.2**	**51.2**												
$[CO_2^-$,CO][e]	66.3	56.6	[f]	[f]	[f]	*48.0*	93.1	79.6	[f]	[f]	[f]	*65.6*	94.6	79.9	[f]	[f]	[f]	*66.8*
						50.2						**68.2**						**69.9**

[a] Values calculated at the B3LYP/6-311+G(d,p) (roman), B3LYP/HW*/6-311+G(d,p) (italics), or B3LYP/Def2TZVP (bold) levels of theory for the lowest energy structure of the given geometry for each metal. Bb = backbone carbonyl, sc = side-chain carbonyl. [b] X = amino nitrogen. [c] X = hydroxyl oxygen. [d] [COOH,CO] structures for Li^+ and Na^+ optimized to [CO,CO] geometries. [e] X = carboxylate oxygen hydrogen bound to NH_3^+. [f] $[CO_2^-$,CO] structures for K^+, Rb^+, and Cs^+ optimized to $[CO_2^-]$ geometries.

of the backbone and forms a hydrogen bond with the carbonyl oxygen of the side chain giving an [N,CO] ground state. The DFT methods, Table 1, find [N,CO]tgtt as the GS, whereas the MP2(full) method finds [N,CO]tcgt to be lowest in energy. An alternate protonation site, between the carbonyl oxygen atoms of the backbone and side chain, [CO,CO], exists at least 27 kJ/mol above the GS. Further details and discussion of the low-energy conformations of H^+(Asn) are available elsewhere.[3]

Comparison of Experimental and Theoretical IR Spectra: Li^+(Asn). Figure 4 compares the experimental IRMPD action spectrum of Li^+(Asn) with calculated IR spectra for the seven low-energy conformers listed in Table 1. Because the theoretical IR intensities are based on single-photon absorption, predictions of IR intensities may not be in direct accordance with the IRMPD action spectrum because the latter is a multiple photon process. Nevertheless, the bands predicted for the ground-state [N,CO,CO]tggt conformer correspond very well with the observed spectrum, in terms of both band position and relative band intensity. The major band observed at 1730 cm^{-1} corresponds to the carbonyl stretch of the backbone COOH group, which explains its large predicted intensity. The band at 1670 cm^{-1} is also a carbonyl stretch but rather originates from the side-chain CO. The latter carbonyl stretch has a lower frequency, both in the complex and free Asn, which is an indication of stronger resonance character within the carboxamide functionality of the side chain. These bands are calculated to red shift by about 43 and 23 cm^{-1}, respectively, upon complexation. Similar features are found in four of the seven low-energy Li^+(Asn) conformations, the exceptions being [N,OH,CO]tggt, [CO,CO]tggt, and $[CO_2^-]$ctgt. In the [N,OH,CO] conformer, the metal cation binds to the hydroxyl group of the backbone rather than the carbonyl, resulting in a blue shift of the carboxylic acid CO stretch back to near its frequency in free Asn. For [CO,CO]tggt, the carboxylic acid CO stretch is red shifted compared to the GS and the [CO,CO]cggt conformer. The difference between the two [CO,CO] structures lies in the orientation of the hydrogen bond of the carboxylic acid hydrogen. In [CO,CO]cggt, this hydrogen interacts with the amino nitrogen, whereas in [CO,CO]tggt, the H bond is formed within the carboxylic acid group, leading to the observed red shift. For the zwitterion, the carboxylate functionality has a CO stretch that is significantly red shifted to 1621 cm^{-1}, whereas the side-chain carbonyl (which is no longer bound to the metal but does bind to the NH_3^+ group) remains at about 1678 cm^{-1}.

The bands observed at about 1415 and 1595 cm^{-1} are found in each of the low-energy spectra because the motions (a C−N stretch and an NH_2 scissors bend, respectively) originate from the side-chain amide group of the ligand, which does not bind to the metal in any of the conformations. In addition to the C−N stretch, the COH bend of the carboxylic acid group has a frequency close to 1415 cm^{-1}, but the IR intensity of this band depends strongly on where the hydroxyl group hydrogen bonds. In [N,CO,CO]tggt, [N,OH,CO]tggt, and [CO,CO]tggt, this group hydrogen bonds to the carbonyl of the carboxylic acid group, whereas in [CO,CO]cggt and [CO,CO]ctgg, it hydrogen bonds to the backbone amino group. This latter conformation gives this motion much more intensity, such that it rivals the carbonyl stretches in the latter two spectra, as also observed previously.[37]

The experimentally observed band at 1160 cm^{-1} is probably the most diagnostic band for the [N,CO,CO]tggt structure. The position and relative intensity of this band is nicely predicted by the IR spectrum for this conformer, whereas no other conformation is predicted to have an isolated, dominant band at this same characteristic frequency. This band corresponds primarily to a bending motion of the COH group of the backbone COOH, H bound to the carbonyl of the same group. At lower frequencies, weak bands at 600, 960−1020, and 1300 cm^{-1} are observed and correlate nicely with the predicted spectrum for [N,CO,CO]tggt, although the spectrum would be even better predicted if bands located in the range of 500−1100

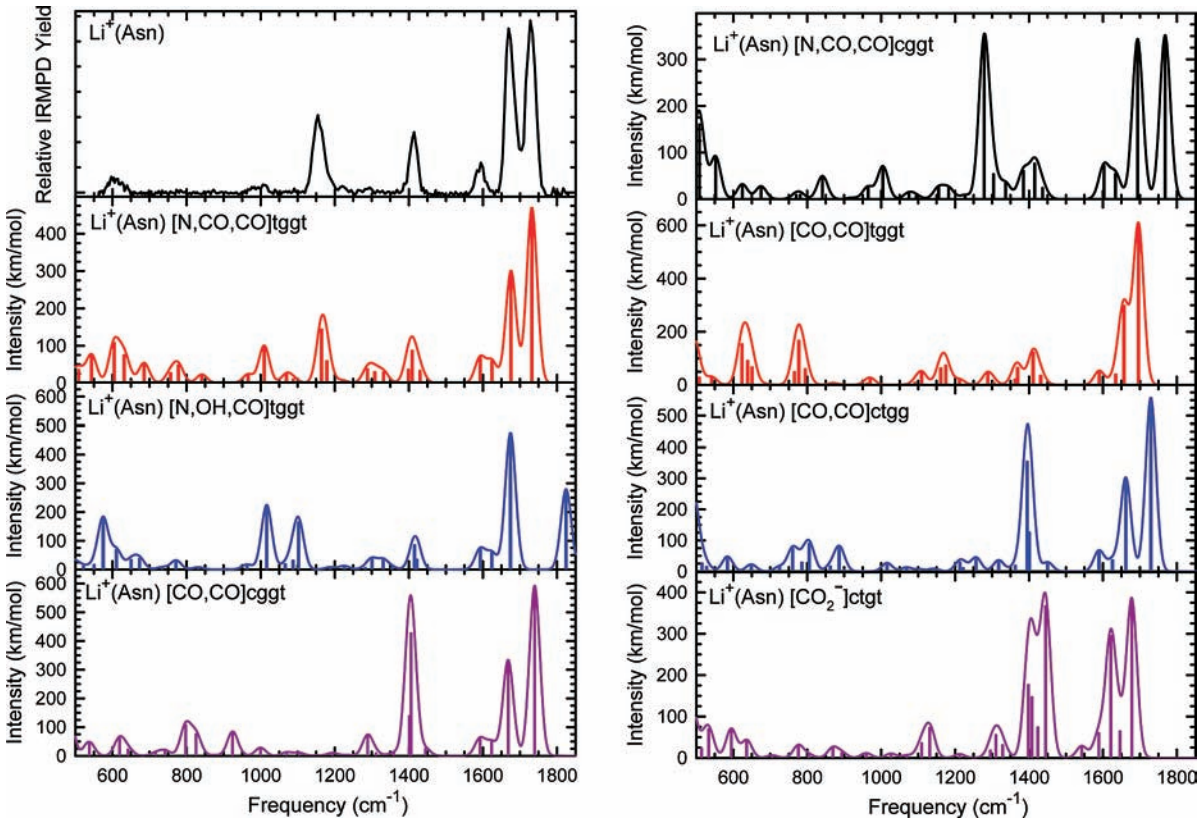

Figure 4. Comparison of the experimental IRMPD action spectrum for Li^+(Asn) with IR spectra for seven conformations predicted at the B3LYP/6-311+G(d,p) level of theory.

and near 1300 cm^{-1} had intensities about one-half of those calculated. These three bands correspond primarily to a wagging motion of the carboxylic acid hydrogen atom of the backbone, a backbone amino umbrella motion, and coupled CH bending motions, respectively. Overall, the Li^+(Asn) spectrum is completely explained by the [N,CO,CO]tggt conformer.

Comparison of Experimental and theoretical IR Spectra: Na^+(Asn). Figure 1 shows that the IRMPD action spectra for Li^+(Asn) and Na^+(Asn) are very similar, exhibiting all of the same major spectral features. Comparison of experimental and theoretical spectra for Na^+(Asn) can be found in Figure S1 of the Supporting Information. There are some subtle differences in the experimental spectra for the two complexes, including a blue shift in the two CO bands, from 1730 to 1740 cm^{-1} and from 1670 to 1675 cm^{-1}. All of the observed features match the calculated spectrum for the [N,CO,CO]tggt conformer of Na^+(Asn), with agreement comparable to that obtained for Li^+(Asn). The calculated spectra correctly predict blue shifts in these two bands of 10 and 7 cm^{-1}, respectively. Likewise the bands at 1160 and 1415 cm^{-1} in the Li^+(Asn) spectrum are red shifted for Na^+(Asn) by 10 and 13 cm^{-1}, respectively, in reasonable agreement with predicted red shifts of 6 and 5 cm^{-1} for [N,CO,CO]tggt. The band at 1590 cm^{-1} shifts little from Li^+(Asn) to Na^+(Asn), which is also in agreement with the predictions for the [N,CO,CO]tggt conformer. In addition, weak bands observed in the Na^+(Asn) spectrum at 550−650, 770, 940−1000, 1090, and 1305 cm^{-1} can all be found in the predicted spectrum for [N,CO,CO]tggt. Only those bands at 770 and 1090 cm^{-1} are not evident in the Li^+(Asn) spectrum. As with Li^+(Asn), the calculated intensities of the bands in the region of 500−1100 and 1300 cm^{-1} are overestimated in intensity compared to the IRMPD spectrum, whereas most of the other bands in the higher frequency region have relative intensities comparable between the calculated and experimental spectra. Relative to the intensities of the major vibrational transitions, the intensities of the weaker bands are enhanced in the Na^+(Asn) spectrum compared to those in the Li^+(Asn) spectrum, even though in both cases it is clear that the [N,CO,CO]tggt conformer can explain all of the spectral features observed. This is a clear indication that strong IR absorptions yield efficient dissociation in both systems, whereas the relative dissociation efficiencies of the more weakly absorbing transitions become enhanced for the more weakly bound Na^+(Asn) molecule. Thus, the appearance of new bands in these cases is not attributable to new conformations but to enhanced sensitivity.

Comparison of Experimental and Theoretical IR Spectra: K^+(Asn) and Rb^+(Asn). The IRMPD action spectrum of K^+(Asn) is similar to that of Na^+(Asn), Figure 1, with peaks at 1095 and 1295 cm^{-1} becoming more obvious and new peaks appearing at 760 and 840 cm^{-1}. In addition, there is retention of the characteristic peaks at 1140, 1400, 1595, 1680, and 1746 cm^{-1}. The appearance of the new bands could be evidence for new conformers or be the result of better sensitivity associated with more facile dissociation of this more weakly bound system. The experimentally measured bond energy for K^+−Asn of 156 ± 7 kJ/mol[2] is substantially weaker than that for Na^+−Asn, 209 ± 6 kJ/mol.[1] The spectrum for Rb^+(Asn) is similar to that for K^+(Asn), Figure 1, with the same new bands compared to the Na^+(Asn) spectrum. Clearly, the ground-state [N,CO,CO]tggt conformation continues to explain the bulk of the observed spectrum for Rb^+(Asn), as can be seen from the comparison in Figure 5. (Comparison of experimental and theoretical spectra for K^+(Asn) can be found in Figure S2 in the Supporting Information). Indeed, the GS [N,CO,CO]tggt conformer is predicted to have bands at 750−770, 843, 1088, and 1280−1300 cm^{-1}, which are all predicted to be relatively

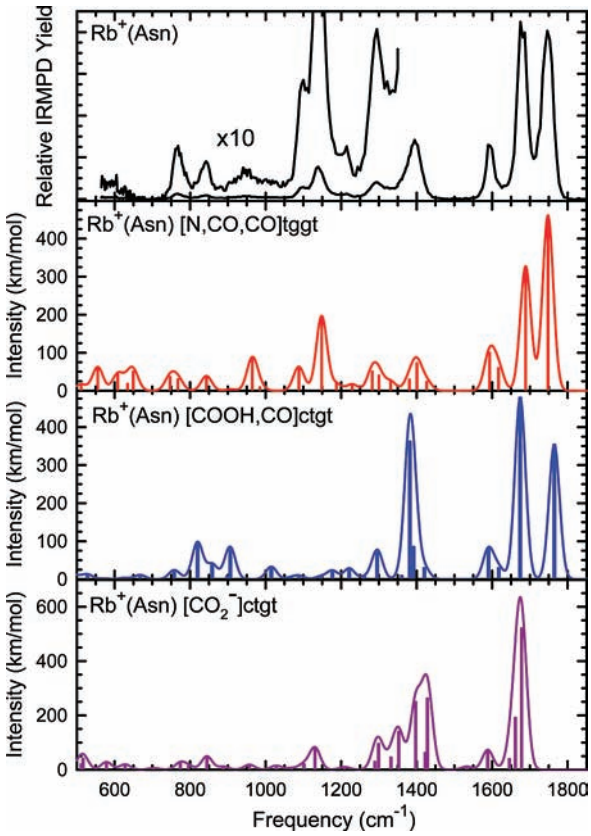

Figure 5. Comparison of the experimental IRMPD action spectrum for Rb^+(Asn) with IR spectra for three low-lying conformations predicted at the B3LYP/HW*/6-311+G(d,p) level of theory.

weak. Their appearance would then be attributed to the increased sensitivity associated with these more weakly bound complexes. However, the [COOH,CO]cggt conformer should also be considered as it is predicted to be low in energy, 4−8 kJ/mol higher than [N,CO,CO]tggt for K^+(Asn) and the [COOH,CO]ctgt conformer is 2.3 kJ/mol lower to 1.4 kJ/mol higher for Rb^+(Asn), Table 1. Figures 5 and S2 (Supporting Information) include theoretical predictions for this conformation along with that for the lowest zwitterionic conformer.

Concentrating on the two high-intensity bands corresponding to the CO stretches, the IRMPD spectra for Rb^+(Asn) [K^+(Asn)] show features at 1680 [1681] and 1746 [1746] cm^{-1} compared to those for Na^+(Asn) at 1675 and 1740 cm^{-1}. Thus, the heavier two alkali cation complexes shift to the blue by about 6 cm^{-1} for both bands and metal cations. The predicted spectrum for [N,CO,CO] predicts blue shifts of 6 [0] and 6 [3] cm^{-1}, in good agreement with observation. In addition, we note that the predicted bands for this conformer are consistently 4 ± 3 cm^{-1} above the observed peak locations for Li^+(Asn) and Na^+(Asn) and are 2 ± 4 cm^{-1} higher for Rb^+(Asn) and K^+(Asn). In contrast, the analogous bands for the [COOH,CO] conformer are predicted to lie at 1674 [1670] and 1765 [1757] cm^{-1}. Now the predicted frequencies of the lower bands are below the observed peak locations by 6 [11] cm^{-1}, and the latter are too high by 19 [11] cm^{-1}, which seems too large a discrepancy. Furthermore, there is no obvious indication of broadening in the higher frequency peak that would be consistent with a mixture of these two conformers. Perhaps the strongest experimental evidence for the [COOH,CO] conformer is that the intensities of the two carbonyl stretch bands, along with the relative intensity of the band at 1400 cm^{-1}, agree reasonably well with those predicted for [COOH,CO] but not with those predicted by the theoretical [N,CO,CO] spectrum.

The dominant features between 1200 and 1800 cm^{-1} in the predicted spectrum for [COOH,CO] overlap directly with the features in the [N,CO,CO] spectrum. Yet the bands at 1300 and 1400 cm^{-1} are distinct in their relative intensities, approximately 1:1 and 1:6 for [N,CO,CO]tggt and [COOH,CO], respectively. A mixture of these two structures could explain the relative experimental intensity observed in the Rb^+(Asn) and K^+(Asn) spectra, about 1:3. The zwitterionic conformer has dominant peaks at 1300 and 1400 cm^{-1} also, but each is contained in a broad feature spanning 1300−1450 cm^{-1}, comprising four dominant bands. Clearly this distinct zwitterionic feature is not dominant in the experimental spectra, although the presence of a small amount of this conformer cannot be ruled out. Another possible diagnostic are the experimental bands at 765 and 842 cm^{-1}, which match the spectral features in the [N,CO,CO] spectrum (predicted bands at 747, 768 [748, 769], and 843 [844] cm^{-1}) much better than the [COOH,CO] spectrum (predicted bands at 820 [815] and 906 [914] cm^{-1}).

In the end, the main arguments in favor of the [COOH,CO] conformer rely on intensities, which are not particularly reliable in comparing theoretical single-photon spectra with experimental multiple-photon spectra. Although some contribution from the [COOH,CO] conformer cannot be ruled out definitively, the frequency comparisons largely suggest that the [N,CO,CO] conformer is dominant for both the Rb^+(Asn) and K^+(Asn) complexes, with no new bands observed compared to Na^+(Asn). These observations strongly suggest that the [N,CO,CO] conformer is the ground state, consistent with the calculations for K^+(Asn), Table 1, and with the B3LYP and MP2(full) results for Rb^+(Asn) but not the B3P86 results. To investigate whether this is a function of the HW* basis set used on Rb, we also examined the relative energies calculated using the LANL08 and Def2SVP basis sets on Rb and the Def2TZVP basis set on all elements. The results are compared in Table 3, where it can be seen that the relative energy of the [COOH,CO] conformer generally increases slightly (by up to 2 kJ/mol) when using these other basis sets. Results for the other conformers also change slightly, by less than 3 kJ/mol in all cases.

Comparison of Experimental and Theoretical IR Spectra: Cs^+(Asn). The IRMPD action spectrum of Cs^+(Asn) clearly presents trends consistent with those observed among the other alkali metal cation, Figure 1. Figure S3 (Supporting Information) compares the experimental spectrum with those calculated for the three most stable conformers. Compared to the Rb^+(Asn) spectrum, no new peaks are observed but the peaks at 760, 840, 1100, and 1300 cm^{-1} are somewhat more pronounced. The retention of the diagnostic features at 1140 and 1400 cm^{-1} indicates that [N,CO,CO] is clearly present. Interestingly, this spectrum looks nearly identical to that of Rb^+(Asn), where the [N,CO,CO] structure can fully explain the spectrum without invoking the [COOH,CO] structure, although contributions from such a conformer cannot be excluded. When using the HW* basis set on Cs, the Cs^+(Asn)[N,CO,CO]tggt structure is low lying but predicted to lie 2−7 kJ/mol *above* the [COOH,CO]ctgt structure at all three levels of theory. Use of the LANL08 basis set on Cs changes these relative energies very little (less than 1 kJ/mol); however, the Def2SVP/6-311+G(2d,2p) and Def2TZVP basis sets lowers the relative energy of the [N,CO,CO] conformer by 2−3 kJ/mol, such that it lies between 0 and 5 kJ/mol above [COOH,CO], Table 3. Likewise, these latter two basis sets lower the relative energy of the zwitterionic [CO_2^-]ctgt conformer by 2−5 kJ/mol but changes the relative energy of the [CO,CO]cggg conformer by less than 1 kJ/mol. Because the experimental spectrum does not appear to be consistent with

TABLE 3: Relative Energies at 0 K (kJ/mol) of Low-Lying Conformers of Cationized Asn Calculated Using Different Basis Sets[a]

complex	structure	HW*/6-311+G(2d,2p)	Def2SVP/6-311+G(2d,2p)	Def2TZVP
Rb^+(Asn)	[N,CO,CO]tggt	0.0, 2.4, 0.0	0.0, 0.5, 0.0	0.0, 1.0, 0.0
	[COOH,CO]ctgt	0.7, 0.0, 1.3	2.7, 0.0, 3.4	2.8, 0.0, 1.7
	[CO_2^-]ctgt	8.7, 6.0, 19.2	8.9, 4.3, 18.4	10.7, 4.9, 16.0
	[CO,CO]cggg	10.9, 12.7, 17.9	12.2, 12.2, 19.3	12.4, 12.7, 18.4
Cs^+(Asn)	[COOH,CO]ctgt	0.0, 0.0, 0.0	0.0, 0.0, 0.0	0.0, 0.0, 0.0
	[N,CO,CO]tggt	3.9, 6.9, 2.6	1.7, 4.5, −0.1	0.8, 4.2, 1.3
	[CO_2^-]ctgt	11.0, 8.9, 20.9	8.5, 6.3, 18.1	8.4, 6.0, 15.5
	[CO,CO]cggg	11.8, 14.2, 16.7	11.0, 13.5, 16.4	10.8, 14.0, 17.2
		HW*/6-311+G(2d,2p)	CRENBL/6-311+G(2d,2p)	Def2TZVP
Ba^{2+}(Asn)	[N,CO,CO]tggt	0.0, 0.0, 0.0	0.0, 0.0, 0.0	0.0, 0.0, 0.0
	[CO_2^-,CO]cgct	15.3, 12.5, 10.2	15.0, 12.4, 8.1	17.1, 14.1, 7.5
	[N,CO,CO]cggt	26.8, 27.1, 27.3	27.5, 27.7, 28.0	27.2, 27.8, 29.0
	[CO,CO]ctgg	30.5, 30.7, 39.0	37.4, 38.6, 49.3	34.4, 35.0, 47.3
	[COOH,CO]cggt	32.2, 28.8, 26.3	43.0, 40.2, 38.1	43.4, 40.2, 37.3
	[CO_2^-]ctgt	33.6, 31.4, 29.0	33.7, 31.5, 31.9	37.3, 34.3, 34.0

[a] Values listed are calculated at the B3LYP, B3P86, and MP2(full) levels of theory using the indicated basis sets. For results obtained using the HW* and CRENBL basis set on Ba, geometries and zero-point energies were calculated at the B3LYP/HW*/6-311+G(d,p) and B3LYP/CRENBL/6-311+G(d,p) levels of theory, respectively. For the Def2TZVP basis set on all elements, geometries and zero-point energies were calculated at the B3LYP/Def2TZVP level.

the [COOH,CO] conformer being a dominant contributor, the larger basis sets on Cs provide a more accurate view of the relative stabilities of the two lowest energy conformers. However, even these basis sets suggest that the [COOH,CO] conformer is the GS, such that this system may provide a theoretical benchmark for developing more accurate basis sets for the heavy metal systems studied here.

Comparison of Experimental and Theoretical IR Spectra: H^+(Asn). The IRMPD action spectrum of H^+(Asn) is unique among the seven systems studied here, as cationization occurs via a covalently bonded proton. Figure 6 compares the experimental spectrum with those calculated for the three most stable conformers. The experimental spectrum exhibits major peaks at about 1777, 1682, 1600, 1400, 1150, and 600 cm^{-1}. The 1777 and 1682 cm^{-1} peaks correspond to carbonyl stretches of the backbone and side chain, respectively. The 1600 cm^{-1} peak corresponds to an NH_2 scissor mode of the side-chain amide nitrogen. The peak at 1400 cm^{-1} is an N−H bend of the backbone H-bonded amino group. Lastly, the 1150 and 600 cm^{-1} bands correspond mostly to OH bending and wagging, respectively, of the hydroxyl in the COOH backbone. All of these peaks are consistent with the two lowest-energy conformers, [N,CO]tgtt and [N,CO]tcgt. Indeed, the different levels of theory disagree on the ground-state energy between these conformers, Table 1. Therefore, both are likely major contributors to the experimental spectrum. However, two minor bands observed at 740 and 830 cm^{-1} suggest that the [N,CO]tgtt structure may be more consistent with the observed spectrum, but the shoulder at 1090 cm^{-1} may be indicative of the [N,CO]tcgt structure. In contrast, the higher-energy [N,CO]ttgt structure exhibits a blue-shifted backbone carbonyl stretch at 1813 cm^{-1}, which is not observed in the experimental spectrum. The shift occurs because this structure forms a hydrogen bond between the protonated amino group and the hydroxyl group of the carboxylic acid, such that the backbone carbonyl is not hydrogen bonded, unlike the two lower energy structures. Thus, the [N,CO]ttgt structure does not appear to be a contributor in the experimental distribution, consistent with its higher theoretical energy.

Comparison of Experimental and Theoretical IR Spectra: Ba^{2+}(Asn). The IRMPD action spectrum of Ba^{2+}(Asn) is noisier and less definitive than those of the alkali metal cation

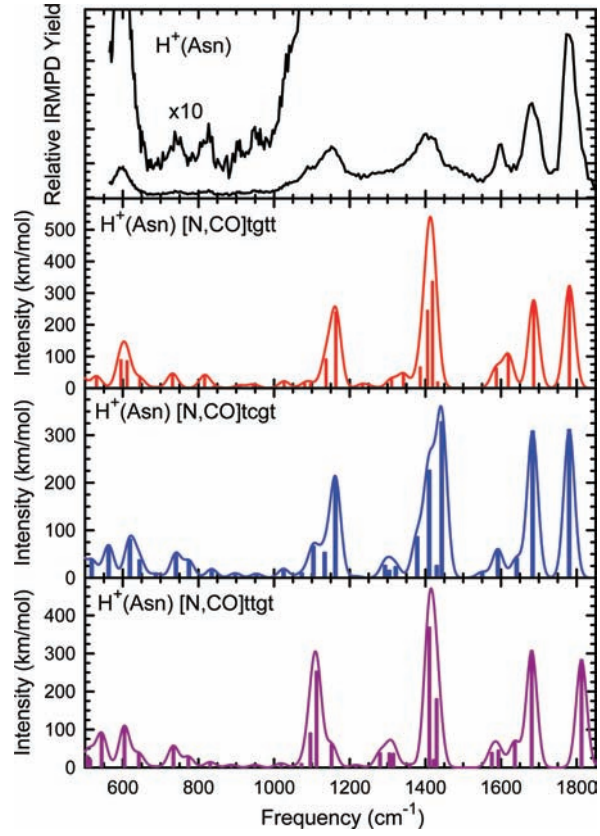

Figure 6. Comparison of the experimental IRMPD action spectrum for H^+(Asn) with IR spectra for three low-lying conformations predicted at the B3LYP/6-311+G(d,p) level of theory.

complexes, Figure 1. Experimentally, this is a result of decreased sensitivity associated with the more challenging dissociation pathways exhibited in this strongly bound, dicationic system. Figure 7 compares the experimental spectrum with those calculated for the three most stable conformers using the Def2TZVP basis set on all elements. Major bands in the experimental spectrum are observed at 1575 cm^{-1} and a broad band ranging from 1640 to 1680 cm^{-1}. The distinct splitting and corresponding shape of these bands correlates well with the predicted spectrum of the GS [N,CO,CO]tggt conformer,

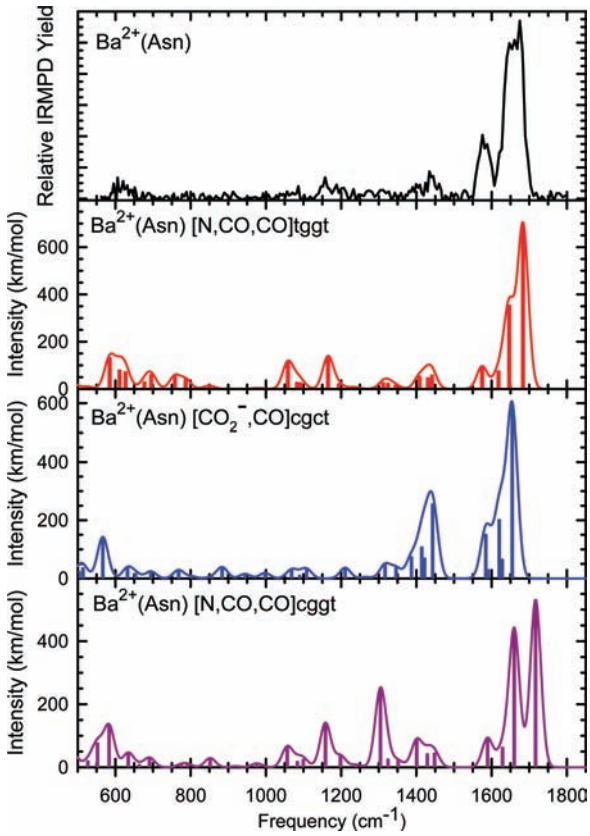

Figure 7. Comparison of the experimental IRMPD action spectrum for Ba^{2+}(Asn) with IR spectra for three low-lying conformations predicted at the B3LYP/Def2TZVP level of theory.

although the [CO_2^-,CO]cgct zwitterionic structure is also similar. Predictions for most of the other conformers (e.g., [N,CO,CO]cggt shown in Figure 7) exhibit greater separation between these major peaks, which in all cases correspond to carbonyl stretches of the side chain and backbone mixed with side-chain NH_2 scissor bending motions. Comparison of the experimental frequencies and those calculated for [N,CO,CO] shows that the two theoretical carbonyl stretches lie about 4 cm^{-1} above the experimental spectrum, the same difference observed between experiment and theory for the alkali metal cations. Calculated spectra performed at the B3LYP/Def2SVP/6-311+G(d,p) and B3LYP/CRENBL/6-311+G(d,p) levels are very similar to that shown for B3LYP/Def2TZVP, whereas B3LYP/HW/6-311+G(d,p) calculations predict these bands are blue shifted by 13−23 cm^{-1} compared to the observed spectrum, which is a larger shift than observed in the analogous bands for the alkali metal cation complexes. Furthermore, the separation between the two bands is predicted to be 37−39 cm^{-1} for Def2TZVP, Def2SVP/6-311+G(d,p), and CRENBL/6-311+G(d,p) compared to 52 cm^{-1} for HW/6-311+G(d,p).

The zwitterionic [CO_2^-,CO]cgct structure is calculated to lie from 7 to 17 kJ/mol above the [N,CO,CO]tggt conformer, Table 3. The carbonyl stretches in this predicted spectrum also agree reasonably well with the observed spectrum, although they are at slightly lower frequencies compared to the experimental spectrum (in contrast to the alkali systems). As a consequence, the side band predicted at 1585 cm^{-1} (compared to 1575 cm^{-1} for the [N,CO,CO] conformer) is not well separated from the more intense carbonyl bands, in contrast to the experimental spectrum.

The minor bands observed in the experimental spectrum at 600, 1155, and 1440 cm^{-1} with hints of bands at 1070 and 1300 cm^{-1} can additionally be correlated to the predicted spectrum for ground-state [N,CO,CO]tggt. The band at 1440 cm^{-1} is also present in the zwitterion spectrum, but the bands near 600, 1070, and 1155 cm^{-1} agree better with the [N,CO,CO] predictions than those for [CO_2^-,CO]. The experimental spectrum contains no evidence for the very strong bands predicted for [N,CO,CO]cggt at 1304 cm^{-1}, [CO,CO]ctgg at 1430 cm^{-1}, [COOH,CO]cggt at 1392 cm^{-1}, [N,OH,CO]tggt at 1050 cm^{-1}, or [CO_2^-] zwitterionic structures near 1400 cm^{-1}. Overall, the experimental spectrum is adequately and accurately described by the single GS [N,CO,CO]tggt conformer, although small contributions from the [CO_2^-,CO] zwitterion cannot be ruled out.

Overall Comparison. We can now provide a more global comparison of the main features in all seven spectra in Figure 1. For the backbone CO stretch in the [N,CO,CO]tggt conformer, the B3LYP/HW*/6-311+G(d,p) predicted frequencies are 1732, 1742, 1745, 1748, and 1749 cm^{-1} for Li^+(Asn)−Cs^+(Asn), respectively, in good agreement with the experimentally observed blue shift of 1730−1750 cm^{-1}, Figure 1. The blue shift for the side-chain CO stretch is somewhat smaller, both theoretically and experimentally, with the predicted frequencies arising at 1676, 1683, 1683, 1689, and 1689 cm^{-1} for Li^+(Asn)−Cs^+(Asn), respectively, and an experimental variation of 1670−1681 cm^{-1}. These blue shifts likely result from decreased perturbations on the CO stretches as the metal cation binding strength decreases. It was noted above that the bands in the Li^+(Asn) spectrum at 1160 and 1415 cm^{-1} shift to the red, reaching 1140 and 1393 cm^{-1} for Cs^+(Asn), respectively. Likewise, the predicted spectral features for the [N,CO,CO]tggt conformer shift from 1164 and 1409 cm^{-1} for Li^+ (Asn) to 1147 and 1401 cm^{-1} for Cs^+(Asn), respectively. This is good agreement for the 1160 cm^{-1} band but underestimates the shift observed for the 1415 cm^{-1} band. This may be some evidence for the presence of the [COOH,CO]cggt conformer, which has a strong band predicted at 1383 cm^{-1} (see, for example, Figure 5), independent of the metal cation. The spectral feature at 1595 cm^{-1} as well as the band at 1300 cm^{-1}, which is only prominent in the spectra for the three heavier alkali metal cations, do not appear to shift among the alkali systems, Figure 1. This is consistent with the predicted trends in these two bands for [N,CO,CO]tggt, which deviate by less than 2 and 4 cm^{-1}, respectively, from K^+(Asn) to Cs^+(Asn). Overall, the predicted trends are in remarkably good agreement with the observed spectra, suggesting that the assignment of these features to the [N,CO,CO]tggt conformation is appropriate. Some evidence for the low-energy [COOH,CO]cggt isomer is present for the heavier alkali cation complexes, but it does not appear to be a dominant contributor. This result contrasts with theoretical predictions that it is the ground-state conformer for Cs^+(Asn), although the larger basis sets on Cs (Def2SVP and Def2TZVP) suggest that it is essentially isoenergetic with the [N,CO,CO]tggt conformer. These conclusions are similar to those for the related alkali cation complexes with glutamine (Gln),[38] which differs from asparagine in having a side chain that is longer by one carbon unit. In agreement with the present study, IRMPD and theoretical studies find that the [N,CO,CO] conformer is favored for the smaller cations and that [CO,CO] and [COOH,CO] structures contribute for the larger cations. As for the present study, no definitive evidence for zwitterionic complexes is found for M^+(Gln).

For H^+(Asn), the experimental IRMPD spectrum is quite similar to those of the alkali metal cation complexes, although most bands are broader, Figure 1. The main distinction is in

the frequency of the highest band, 1775 cm^{-1} for H^+(Asn) compared to 1730−1752 cm^{-1} for the alkali complexes. This band corresponds to the carbonyl stretch of the backbone. This carbonyl binds directly with the alkali metal cations but in the [N,CO] structures of H^+(Asn) is more weakly hydrogen bonded to the protonated amino group, r(NH···OC) = 2.252 and 2.083 Å in the tgtt and tcgt conformers, respectively. In contrast, the hydrogen bond to the side-chain carbonyl is 1.606 and 1.608 Å, respectively, such that this stretch is perturbed comparably with the alkali metal complexes. As discussed above, a mixture of the two ground-state [N,CO] structures is consistent with all observed bands.

Ba^{2+}(Asn) displays the most distinctive spectrum among those examined here. Spectral results for Ba^{2+}(Asn) find the backbone and side-chain CO stretches have frequencies more alike to one another and more strongly red shifted than those for the alkali metal complexes. The vibrational similarity and red shift result from tighter binding to the doubly charged metal cation compared to the singly charged metal complexes. Because of its 2-fold charge, the atomic radius of Ba^{2+} falls near that of K^+, such that its structural characteristics more closely mimic those of K^+(Asn) rather than Rb^+(Asn) and Cs^+(Asn), and the relative energies of various conformers is comparable to Li^+(Asn) and Na^+(Asn). Indeed, the Ba^{2+}(Asn) spectrum is most consistent with a single [N,CO,CO]tggt conformation, although contributions from a tridentate [CO_2^-,CO] zwitterionic conformation cannot be ruled out. To our knowledge, Asn is the first amino acid that appears not to take on a zwitteronic structure in complexation with Ba^{2+} in the gas phase, whereas Gly,[39−42] Trp,[43] Arg, Gln, Pro, Ser, Val,[32] and Glu,[44] all form zwitterionic structures when complexed to Ba^{2+}.

Conclusions

IRMPD action spectra of cationized asparagine in the region of 550−1800 cm^{-1} have been obtained for complexes with Li^+, Na^+, K^+, Rb^+, Cs^+, Ba^{2+}, and H^+. Comparison with IR spectra calculated at the B3LYP/6-311+G(d,p) (Li^+, Na^+, K^+, and H^+ complexes), B3LYP/HW*/6-311+G(d,p) (Rb^+ and Cs^+complexes), and B3LYP/Def2TZVP (Ba^{2+} complexes) levels of theory allow conformations present in the experiment to be identified. The experimental results suggest that only the tridentate [N,CO,CO] conformation is present for the Li^+(Asn) and Na^+(Asn) complexes, in agreement with the predicted ground states of these complexes. For the K^+(Asn), Rb^+(Asn), and Cs^+(Asn) complexes, the tridentate [N,CO,CO] conformer continues to dominate, although contributions from the [COOH,CO] conformer cannot be ruled out. No definitive evidence for zwitterionic conformers, [CO_2^-], is found. Theory finds that the [COOH,CO] conformer becomes the ground state for the heavier alkali metal systems; however, the spectra do not appear to be consistent with the [COOH,CO] conformer being a dominant contributor. Therefore, this system may provide a benchmark for assessing accurate basis sets for these heavy metal systems.

For H^+(Asn), a mixture of two comparable [N,CO] structures appear to dominate the spectrum. Results for the complex of Asn with Ba^{2+} suggest that because its 2-fold higher charge density leads to an atomic radius similar to K^+, its structural characteristics more closely mimic those of Na^+(Asn) and K^+(Asn) rather than Rb^+(Asn) and Cs^+(Asn). Indeed, the Ba^{2+}(Asn) spectrum is consistent with a single [N,CO,CO] conformation. In this system, theory using the HW/6-311+G(d,p) basis set underestimates the perturbation of metal cation binding to the carbonyl stretches, whereas the Def2SVP, Def2TZVP, and CRENBL basis sets provide results in good agreement with experiment. In no case do we find our cationized Asn complexes to provide evidence for a dominant population of a zwitterionic structure, distinguishing Asn as the first known amino acid *not* to have a ground-state zwitteron in complexation with Ba^{2+} in the gas phase.[32,39−44]

Acknowledgment. This work is part of the research program of FOM, which is financially supported by the Nederlandse Organisatie voor Wetenschappelijk Onderzoek (NWO). Additional financial support was provided by the National Science Foundation, Grants PIRE-0730072, CHE-0748790, and CHE-0649039. The skillful assistance of the FELIX staff is gratefully acknowledged.

Supporting Information Available: Three figures showing a comparison between the experimental IRMPD spectrum and theoretically predicted IR spectra of low-lying conformations of Na^+(Asn), K^+(Asn), and Cs^+(Asn); three tables (S1−S3) providing the vibrational frequencies and IR intensities for the [N,CO,CO]tggt, [COOH,CO], or [CO,CO] and [CO_2^-] or [CO_2^-,CO] conformations for M^+(Asn) calculated at the B3LYP/6-311+G(d,p) (M^+ = Li^+, Na^+, and K^+), B3LYP/HW*/6-311+G(d,p) (M^+ = Rb^+ and Cs^+), or B3LYP/Def2TZVP (M^+ = Ba^{2+}) levels of theory; one table (S4) providing the vibrational frequencies and IR intensities for alternative conformations of Li^+(Asn) calculated at the B3LYP/6-311+G(d,p) and Ba^{2+}(Asn) calculated at the B3LYP/Def2TZVP level of theory; one table (S5) providing the vibrational frequencies and IR intensities for conformations of H^+(Asn) calculated at the B3LYP/6-311+G(d,p) level of theory. This material is available free of charge via the Internet at http://pubs.acs.org.

References and Notes

(1) Heaton, A. L.; Moision, R. M.; Armentrout, P. B. *J. Phys Chem. A* **2008**, *112*, 3319.
(2) Heaton, A. L.; Armentrout, P. B. *J. Phys. Chem. B* **2008**, *112*, 12056.
(3) Heaton, A. L.; Armentrout, P. B. *J. Am. Soc. Mass Spectrom.* **2009**, in press.
(4) Heaton, A. L.; Ye, S. J.; Armentrout, P. B. *J. Phys. Chem. A* **2008**, *112*, 3328.
(5) Heaton, A. L.; Armentrout, P. B. *J. Am. Chem. Soc.* **2008**, *130*, 10227.
(6) Robinson, N. E.; Robinson, A. B. *Proc. Natl. Acad. Sci. U.S.A.* **2001**, *98*, 944.
(7) Valle, J. J.; Eyler, J. R.; Oomens, J.; Moore, D. T.; van der Meer, A. F. G.; von Heldon, G.; Meijer, G.; Hendrickson, C. L.; Marshall, A. G.; Blakney, G. T. *Rev. Sci. Instrum.* **2005**, *76*, 023103.
(8) Polfer, N. C.; Oomens, J.; Moore, D. T.; von Helden, G.; Meijer, G.; Dunbar, R. C. *J. Am. Chem. Soc.* **2006**, *128*, 517.
(9) Polfer, N. C.; Oomens, J. *Phys. Chem. Chem. Phys.* **2007**, *9*, 3804.
(10) Mize, T. H.; Taban, I.; Duursma, M.; Seynen, M.; Konijnenburg, M.; Vijftigschild, A.; Doornik, C. V.; Rooij, G. V.; Heeren, R. M. A. *Int. J. Mass Spectrom.* **2004**, *235*, 243.
(11) Oepts, D.; van der Meer, A. F. G.; van Amersfoort, P. W. *Infrared Phys. Technol.* **1995**, *36*, 297.
(12) Moision, R. M.; Armentrout, P. B. *J. Phys. Chem. A* **2002**, *106*, 10350.
(13) Pearlman, D. A.; Case, D. A.; Caldwell, J. W.; Ross, W. R.; Cheatham, T. E.; DeBolt, S.; Ferguson, D.; Seibel, G.; Kollman, P. *Comput. Phys. Commun.* **1995**, *91*, 1.
(14) Bylaska, E. J.; de Jong, W. A.; Kowalski, K.; Straatsma, T. P.; Valiev, M.; Wang, D.; Aprà, E.; Windus, T. L.; Hirata, S.; Hackler, M. T.; Zhao, Y.; Fan, P.-D.; Harrison, R. J.; Dupuis, M.; Smith, D. M. A.; Nieplocha, J.; Tipparaju, V.; Krishnan, M.; Auer, A. A.; Nooijen, M.; Brown, E.; Cisneros, G.; Fann, G. I.; Früchtl, H.; Garza, J.; Hirao, K.; Kendall, R.; Nichols, J. A.; Tsemekhman, K.; Wolinski, K.; Anchell, J.; Bernholdt, D.; Borowski, P.; Clark, T.; Clerc, D.; Dachsel, H.; Deegan, M.; Dyall, K.; Elwood, D.; Glendening, E.; Gutowski, M.; Hess, A.; Jaffe, J.; Johnson, B.; Ju, J.; Kobayashi, R.; Kutteh, R.; Lin, Z.; Littlefield, R.; Long, X.; Meng, B.; Nakajima, T.; Niu, S.; Pollack, L.; Rosing, M.; Sandrone, G.; Stave, M.; Taylor, H.; Thomas, G.; Lenthe, J. v.; Wong, A.;

Zhang, Z. *Nwchem a Computational Chemistry Package for Parallel Computers*, Version 4.5Ed.; Pacific Northwest National Laboratory: Richland, WA, 2003.

(15) Roothaan, C. C. *Rev. Mod. Phys.* **1951**, *23*, 69.

(16) Binkley, J. S.; Pople, J. A.; Hehre, W. J. *J. Am. Chem. Soc.* **1980**, *102*, 939.

(17) Frisch, M. J.; Trucks, G. W.; Schlegel, H. B.; Scuseria, G. E.; Robb, M. A.; Cheeseman, J. R.; Montgomery, J. A., Jr.; Vreven, T.; Kudin, K. N.; Burant, J. C.; Millam, J. M.; Iyengar, S. S.; Tomasi, J.; Barone, V.; Mennucci, B.; Cossi, M.; Scalmani, G.; Rega, N.; Petersson, G. A.; Nakatsuji, H.; Hada, M.; Ehara, M.; Toyota, K.; Fukuda, R.; Hasegawa, J.; Ishida, M.; Nakajima, T.; Honda, Y.; Kitao, O.; Nakai, H.; Klene, M.; Li, X.; Knox, J. E.; Hratchian, H. P.; Cross, J. B.; Adamo, C.; Jaramillo, J.; Gomperts, R.; Stratmann, R. E.; Yazyev, O.; Austin, A. J.; Cammi, R.; Pomelli, C.; Ochterski, J. W.; Ayala, P. Y.; Morokuma, K.; Voth, G. A.; Salvador, P.; Dannenberg, J. J.; Zakrzewski, V. G.; Dapprich, S.; Daniels, A. D.; Strain, M. C.; Farkas, O.; Malick, D. K.; Rabuck, A. D.; Raghavachari, K.; Foresman, J. B.; Ortiz, J. V.; Cui, Q.; Baboul, A. G.; Clifford, S.; Cioslowski, J.; Stefanov, B. B.; Liu, G.; Liashenko, A.; Piskorz, P.; Komaromi, I.; Martin, R. L.; Fox, D. J.; Keith, T.; Al-Laham, M. A.; Peng, C. Y.; Nanayakkara, A.; Challacombe, M.; Gill, P. M. W.; Johnson, B.; Chen, W.; Wong, M. W.; Gonzalez, C.; Pople, J. A. *Gaussian 03*, Revision B.02; Gaussian, Inc.: Pittsburgh, PA, 2003.

(18) Becke, A. D. *J. Chem. Phys.* **1993**, *98*, 5648.

(19) Ditchfield, R.; Hehre, W. J.; Pople, J. A. *J. Chem. Phys.* **1971**, *54*, 724.

(20) McLean, A. D.; Chandler, G. S. *J. Chem. Phys.* **1980**, *72*, 5639.

(21) Krishnan, R.; Binkley, J. S.; Seeger, R.; Pople, J. A. *J. Chem. Phys.* **1980**, *72*, 650.

(22) Moision, R. M.; Armentrout, P. B. *Phys. Chem. Chem. Phys.* **2004**, *6*, 2588.

(23) Armentrout, P. B.; Rodgers, M. T.; Oomens, J.; Steill, J. D. *J. Phys. Chem. A* **2008**, *112*, 2248.

(24) Rodgers, M. T.; Armentrout, P. B.; Oomens, J.; Steill, J. D. *J. Phys. Chem. A* **2008**, *112*, 2258.

(25) Foresman, J. B.; Frisch, A. E. *Exploring Chemistry with Electronic Structure Methods*, 2nd ed.; Gaussian Inc.: Pittsburgh, PA, 1996.

(26) Hay, P. J.; Wadt, W. R. *J. Chem. Phys.* **1985**, *82*, 299.

(27) Glendening, E. D.; Feller, D.; Thompson, M. A. *J. Am. Chem. Soc.* **1994**, *116*, 10657.

(28) Weigend, F.; Ahlrichs, R. *Phys. Chem. Chem. Phys.* **2005**, *7*, 3297.

(29) Leininger, T.; Nicklass, A.; Kuechle, W.; Stoll, H.; Dolg, M.; Bergner, A. *Chem. Phys. Lett.* **1996**, *255*, 274.

(30) Kaupp, M.; Schleyer, P. V.; Stoll, H.; Preuss, H. *J. Chem. Phys.* **1991**, *94*, 1360.

(31) Ross, R. B.; Powers, J. M.; Atashroo, T.; Ermler, W. C.; Lajohn, L. A.; Christiansen, P. A. *J. Chem. Phys.* **1990**, *93*, 6654.

(32) Bush, M. F.; Oomens, J.; Saykally, R. J.; Williams, E. R. *J. Am. Chem. Soc.* **2008**, *130*, 6463.

(33) Feller, D. *J. Comput. Chem.* **1996**, *17*, 1571.

(34) Schuchardt, K. L.; Didier, B. T.; Elsethagen, T.; Sun, L.; Gurumoorthi, V.; Chase, J.; Li, J.; Windus, T. L. *J. Chem. Inf. Model.* **2007**, *47*, 1045.

(35) Polfer, N. C.; Oomens, J.; Dunbar, R. C. *Phys. Chem. Chem. Phys.* **2006**, *8*, 2744.

(36) Wilson, R. G.; Brewer, G. R. *Ion Beams with Applications to Ion Implantation*; Wiley: New York, 1973.

(37) Bakker, J. M.; MacAleese, L.; Meijer, G.; von Helden, G. *Phys. Rev. Lett.* **2003**, *91*, 203003.

(38) Bush, M. F.; Oomens, J.; Saykally, R. J.; Williams, E. R. *J. Phys. Chem. A* **2008**, *112*, 8578.

(39) Strittmatter, E. F.; Lemoff, A. S.; Williams, E. R. *J. Phys. Chem. A* **2000**, *104*, 9793.

(40) Hoyau, S.; Pelicier, J.-P.; Rogalewicz, F.; Hoppilliard, Y.; Ohanessian, G. *Eur. J. Mass Spectrom* **2001**, *7*, 303.

(41) Ai, H.; Bu, Y.; Li, P. *Int. J. Quantum Chem.* **2003**, *94*, 205.

(42) Ai, H.; Bu, Y.; Li, P.; Zhang, C. *New J. Chem.* **2005**, *29*, 1540.

(43) Dunbar, R. C.; Polfer, N. C.; Oomens, J. *J. Am. Chem. Soc.* **2007**, *129*, 14562.

(44) O'Brien, J. T.; Prell, J. S.; Steill, J. D.; Oomens, J.; Williams, E. R. *J. Phys. Chem. A* **2008**, *112*, 10823.

JP9008064